ACS APPLIED MATERIALS & INTERFACES

Research Article

www.acsami.org

Biological Activity of Mesoporous Dendrimer-Coated Titanium Dioxide: Insight on the Role of the Surface−Interface Composition and the Framework Crystallinity

Katarzyna Milowska,[†] Aneta Rybczyńska,[†] Joanna Mosiolek,[†] Joanna Durdyn,[†] Eligia M. Szewczyk,[‡] Nadia Katir,[§] Younes Brahmi,[∥] Jean-Pierre Majoral,[⊥] Mosto Bousmina,[§] Maria Bryszewska,[†] and Abdelkrim El Kadib*[,§]

[†]Department of General Biophysics, Faculty of Biology and Environmental Protection, University of Lodz, 141/143 Pomorska Street, 90-236 Lodz, Poland

[‡]Department of Pharmaceutical Microbiology and Microbiological Diagnostics, Medical University of Lodz, 137 Pomorska Street, 90-235 Lodz, Poland

[§]Euromed Research Center, Engineering Division, Euro-Mediterranean University of Fes (UEMF), Fès-Shore, Route de Sidi Hrazem, 30070 Fès, Morocco

[∥]Université Mohammed V Agdal, Faculté des Sciences, and MAScIR foundation, 10100 Rabat, Morocco

[⊥]Laboratoire de Chimie de Coordination (LCC) CNRS, 205 route de Narbonne, 31077 Toulouse, France

Supporting Information

ABSTRACT: Hitherto, the field of nanomedicine has been overwhelmingly dominated by the use of mesoporous organosilicas compared to their metal oxide congeners. Despite their remarkable reactivity, titanium oxide-based materials have been seldom evaluated and little knowledge has been gained with respect to their "structure−biological activity" relationship. Herein, a fruitful association of phosphorus dendrimers (both "ammonium-terminated" and "phosphonate-terminated") and titanium dioxide has been performed by means of the sol−gel process, resulting in mesoporous dendrimer-coated nanosized crystalline titanium dioxide. A similar organo-coating has been reproduced using single branch-mimicking dendrimers that allow isolation of an amorphous titanium dioxide. The impact of these materials on red blood cells was evaluated by studying cell hemolysis. Next, their cytotoxicity toward B14 Chinese fibroblasts and their antimicrobial activity were also investigated. Based on their variants (cationic versus anionic terminal groups and amorphous versus crystalline titanium dioxide phase), better understanding of the role of the surface−interface composition and the nature of the framework has been gained. No noticeable discrimination was observed for amorphous and crystalline material. In contrast, hemolysis and cytotoxicity were found to be sensitive to the nature of the interface composition, with the ammonium-terminated dendrimer-coated titanium dioxide being the most hemolytic and cytotoxic material. This surface-functionalization opens the door for creating a new synergistic machineries mechanism at the cellular level and seems promising for tailoring the biological activity of nanosized organic−inorganic hybrid materials.

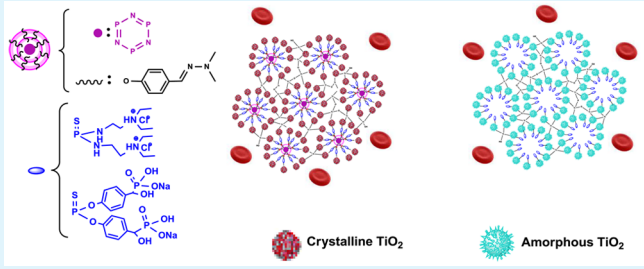

KEYWORDS: *phosphorus dendrimers, titanium dioxide, crystalline material, amorphous material, hemolysis, cytotoxicity*

1. INTRODUCTION

Titanium-based materials have been used in the field of orthopedic implants since the 1970s. Owing to their well-established mechanical strength, low density, excellent resistance to corrosion, and lack of cytotoxicity effect, bulk titanium, titanium-based alloys, and titanium dioxide systems are nowadays among the most common implant materials in diverse applications, including cardiovascular stents, joint replacement, and dental implants.[1,2] In parallel, the advent of nanotechnology and its invaluable opportunities for health care allowed a strong intrusion of mesoporous functional materials to the field of nanomedicine with a conceptual rethinking of the way of fixing pharmaceuticals to the human bodies.[3,4] The most ubiquitous tool in this category is the mesoporous silica and its unlimited surface functional congeners.[5−8] The wealth of available precursors as well as the versatility and flexibility in their synthesis afforded a rich library for exhaustive screening of biocandidates spanning from simple exotic chemicals to more sophisticated drug-delivery transporters, multifunctional theranostic carriers, and extra-stimulus biodegradable biomateri-

Received: June 1, 2015
Accepted: August 25, 2015
Published: August 25, 2015

DOI: 10.1021/acsami.5b04780
ACS Appl. Mater. Interfaces 2015, 7, 19994−20003

als.[9−12] While our understanding has significantly progressed with silica, and in spite of its minimal allure compared to other metal oxides, only a limited basic knowledge has been gained with nonsiliceous metal oxide materials.[13−16] Of those privileged in this category, titanium dioxide is undoubtedly the most remarkable one, offering broad possibilities thanks to its chemical reactivity,[17,18] enhanced stability,[19−21] versatility in chemical composition and crystallinity,[22] and its photocatalytic activity,[23] being certainly the most important feature and at the basis of its implementation as an outstanding photo-oxidation catalyst. Indeed, high-surface-area titanium dioxide-based materials can offer valuable alternatives to functional organo-silica materials, considering their ability to do a similar task with additional possibilities of using their photochemical reactivity for, among others, photodynamic therapy.[24,25] The paucity of biomedical investigations on titanium dioxide-based materials finds its roots in (i) the difficulties in preparing high-surface-area mesoporous titanium dioxide in comparison to silica[26,27] (the main issue is to reconciliate the two antagonistic features "mesoporosity and crystallinity" as the crystal growth naturally induces a dramatic collapse of the open framework and destroys its porosity[26−28]); (ii) the less-explored engineering of titanium dioxide surface functionalization whereas the silica modification reaches a high level of maturity[7,29,30]); (iii) the complicated morphologies of titanium dioxide (amorphous versus crystalline) and the existence of several allotropic phases (anatase, brookite, rutile), thereby hampering a rational correlation of the structure−bioactivity relationship.[31]

We recently discovered that some challenging aspects of titanium alkoxide mineralization could be solved by the use of phosphorus dendrimers as amphiphilic nanoreactors.[32,33] Specifically, discrete anatase nanoparticles of ∼5 nm entangled in a mesoporous network were accessible by thermal-free and even hydrothermal-free sol−gel synthetic mineralization at a moderate temperature of 60 °C. By sharp contrast, the use of branch-mimicking dendrimers (isolated single molecules featuring similar reactive-surface chemistry) as organo-modifiers during the sol−gel mineralization allowed only the isolation of amorphous titanium dioxide phase. Indeed, these antagonistic synthetic procedures afford for the first time comparable materials in terms of their surface−interface composition (attained by the use of similar terminal organo-modifiers) and hydroxyl surface condensation (by operating under similar sol−gel temperature of 60 °C) but with different inorganic substructures (amorphous versus crystalline one). Besides, phosphorus dendrimers are a class of novel nano building blocks with a wide range of potential applications in medicinal chemistry[34,35] and materials science.[36] The sequential presence of phosphorus element at the core, within the cascade skeletal, and on the terminal surface make these hyperbranched macromolecules particularly important for interactions with biological systems.[37] The last two decades in particular have witnessed an avalanche of research for their utilization as cargo as well as their activity per se.[38] In light of their virtues, the association of phosphorus dendrimers and titanium dioxide within the same building block—hitherto unexplored—seems very promising to create new synergistic machineries mechanisms at the cellular level. The promising combination of these dissimilar organic and mineral phases and the uniqueness of their variants prompted us to engage in profound studies on their biological activity. In this contribution, we report our preliminary biological assessments based on the hemolytic activity, cytotoxicity and antimicrobial activity, aiming at deeply understanding the role of the surface−interface composition and that of the nature (amorphous versus crystalline) of the material's framework.

2. EXPERIMENTAL SECTION

General. ^{13}C and ^{31}P CP MAS NMR spectra were acquired on a Bruker Avance 400 WB spectrometer operating at 100 and 162 MHz, respectively, under cross-polarization conditions. Nitrogen sorption isotherms at 77 K were obtained with a Micromeritics ASAP 2010 apparatus. Prior to measurement, the samples were degassed for 8 h at 120 °C. The surface area (S_{BET}) was determined from BET treatment in the range 0.04−0.3 p/p_0 assuming a surface coverage of the nitrogen molecule estimated to be 13.5 Å. X-ray powder diffraction (XRD) patterns were recorded on a D8 Advance Bruker AXS system using Cu Kα radiation with a step size of 0.02° in the 2θ range from 0.3 to 10° for SAXS, and from 0.45 to 87° for WAXS (geometry: Bragg-Brentano, $\theta/2\theta$ mode). DRUV spectra were measured in the 200−800 nm range using Spectralon as the reference on a PerkinElmer Lambda 1050 spectrometer equipped with an integrating sphere (Lapshere, North Sutton, USA). Scanning electronic microscopy (SEM) images were obtained using a JEOL JSM 6700F. Transmission electronic microscopy (TEM) images were obtained using JEOL JEM 2010 at an activation voltage of 200 kV.

Materials. Dimethyl sulfoxide (DMSO), phosphate buffered saline (PBS) tablets, fetal bovine serum, and trypsin were purchased from Sigma-Aldrich (USA). All other chemicals used were of analytical grade. All solutions were prepared using water purified by the Mili-Q system. Two dendrimers of the fourth generation, labeled hereafter as **DG_4**, were designed for this study. These dendrimers are built from a cyclotriphosphazene core, repetitive bricks of branching units and either terminal ammoniums (**DG_4-NH^+**) or phosphonic acid sodium salts (**DG_4-PO^-**). In parallel, branch-mimicking dendrimers consisting of single molecules with the same terminated ammoniums (**B-NH^+**) or phosphonate (**B-PO^-**) were prepared in order to accurately reproduce the same interface−surface composition. These starting materials were prepared according to the literature procedure.[33] The chemical structures of these organo-modifiers (either dendrimers or their branch-mimicking congeners) are shown in the Supporting Information (S1, ESI).

Preparation of Materials. A functional dendrimer phosphonate (**DG_4-PO^-Na^+**) and ammonium (**DG_4-NH^+Cl^-**) were solubilized in water/ethanol (2/5 v/v) solution. After 15 min of stirring, titanium isopropoxide precursor in a given molar ratio [**D**]:[Ti] = 1:20, was added to the transparent dendritic solution at room temperature. Upon addition, the resulting solution was heated at 60 °C for 10 h. After filtration and extensive washing of the precipitate with ethanol, the collected solid was dried at 60 °C for 2 h.

Zeta Potential Measurements. The measurements of the zeta potential (electrokinetic potential) were performed with Zetasizer Nano ZS from Malvern Instruments (UK), which uses electrophoresis and LDV (Laser Doppler Velocimetry) techniques. Applying a combination of these two techniques allowed measuring the electrophoretic mobility of the molecules in solution. Results were obtained 10 times with the zero field correction. The zeta potential value was calculated directly from the Helmholtz−Smoluchowski equation using the Malvern software.[39] The measurements of nanoparticles zeta potential at the concentration of 1, 5, and 10 $\mu g.mL^{-1}$ were performed in phosphate buffer at pH = 7.4. The results were averaged.

Measurement of the Hydrodynamic Diameter. The particle sizes were measured using dynamic light scattering (DLS) in a photon correlation spectrometer (Zetasizer Nano-ZS, Malvern Instruments, UK).[40] Samples in 10 mM PBS, pH 7.4 were placed in the plastic cells DTS0012 (Malvern) and measured at 37 °C. The data were analyzed using the Malvern software.

Cytotoxicity Assay. Chinese hamster cells (B14 cell line) were purchased from Child Health Centre in Warsaw (Poland). Cells were grown as a monolayer in DMEM medium supplemented with 10% fetal bovine serum with 100 units/mL gentamycin. The cells were

DOI: 10.1021/acsami.5b04780
ACS Appl. Mater. Interfaces 2015, 7, 19994−20003

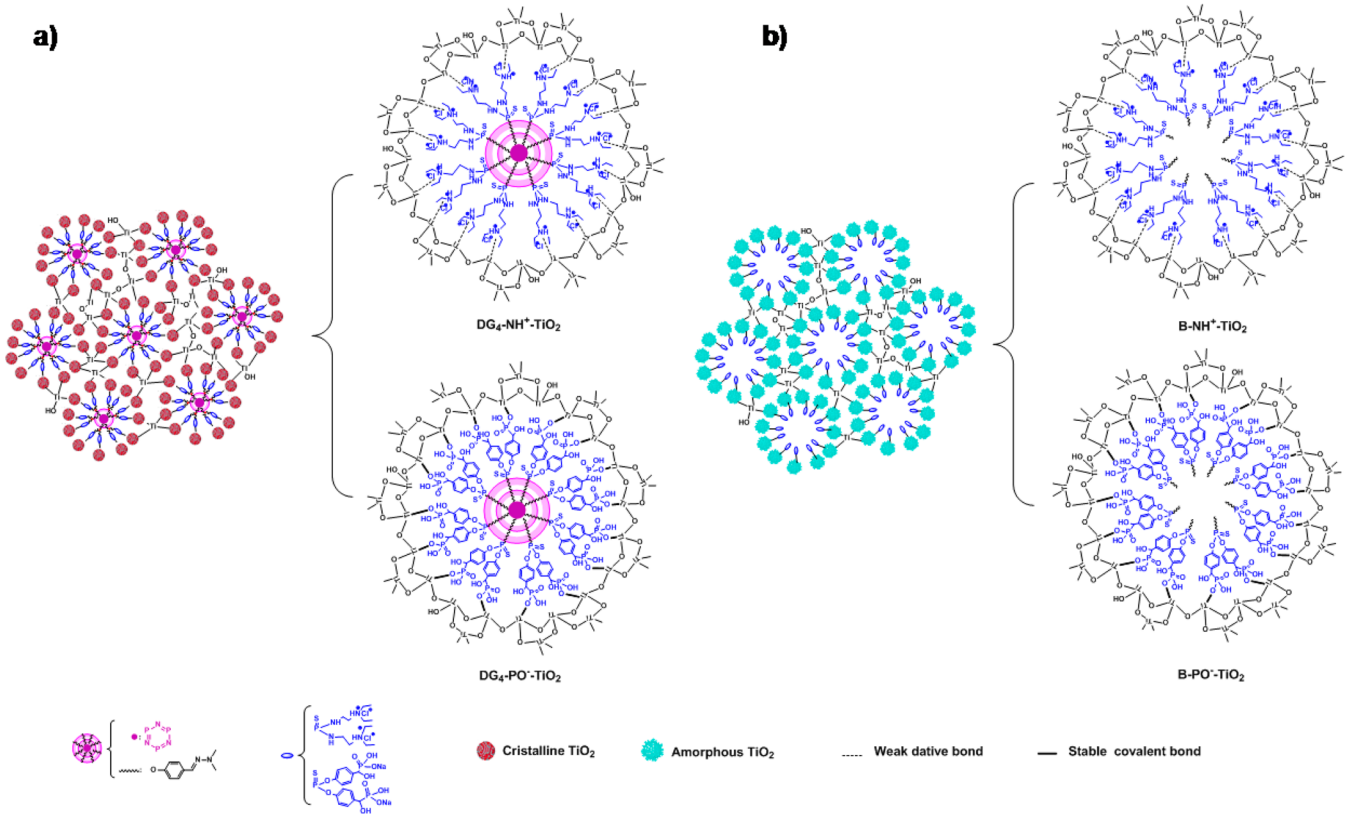

Figure 1. Schematic representation of the periodicity of the as-prepared organic−inorganic materials and their interface composition. (a) Dendrimer-coated titanium dioxide results in a crystalline anatase phase. (b) Branch-mimicking dendrimer-coated titanium dioxide is built from an amorphous framework. Elucidation in each material of the interface composition (both ammonium-terminated and phosphonate-terminated) where dative bonds link the former to the titanium oxide phase while the latter forms a stable covalent bridge with the mineral phase.

maintained at 37 °C in an atmosphere of 5% CO_2 and 95% air with more than 95% humidity. Cells were split for subcultures every 2 days.

Cell viability was measured by the MTT assay.[41] The test is based on the reduction of the soluble yellow MTT tetrazolium salt to a blue, insoluble formazan produced by mitochondrial succinate dehydrogenase. The amount of formazan produced is proportional to the number of living cells. Cells were seeded at a density of 2.0×10^5/well into 96-well microtitrate plates using DMEM medium. They were treated with nanoparticles at 37 °C in a 5% carbon dioxide−95% air atmosphere for 24 h, and recovered by gentle washing with PBS (pH = 7.4) twice. After incubation, 50 μL of 3-[4,5-dimethylthiazol-2-yl]-2,5-diphenyltetrazolium bromide (MTT) solution was added to each well, followed by 3 h of incubation. Next, MTT-containing medium was removed, and 100 μL of DMSO was added to each well to dissolve formazan crystals. Absorbance of the converted dye was measured at 570 nm using a microplate spectrophotometer (BioTek). Cell viability was calculated as the percent ratio of absorbance of the samples to the referent control. Control was 100%.

Hemotoxicity. Blood from healthy donors was obtained from Central Blood Bank in Lodz. Blood was anticoagulated with 3% sodium citrate. Erythrocytes were separated from blood plasma and leukocytes by centrifugation (4000*g*, 10 min) at 4 °C and washed three times with PBS (phosphate buffered saline; pH = 7.4). Erythrocytes were used immediately after isolation.

To study the effect of nanoparticles containing titanium dioxide on erythrocytes, nanoparticles were added in the concentrations range of 0.1−100 $\mu g \cdot mL^{-1}$ to red blood cells of 2% hematocrit and incubated at 37 °C for 24 h. After incubation, suspensions were centrifuged (1000*g*, 10 min). Hemolysis was determined by measuring the hemoglobin content in the supernatant at 540 nm.

The percentage of hemolysis was calculated from the formula

$$\%\text{hemolysis} = (A/A_c) \times 100\%$$

where A represents the absorbance of the sample, and A_c is the absorbance of the sample in water (100% hemolysis).

Morphological Changes. Morphology of erythrocytes was evaluated by microscopic observation. The final concentrations of nanoparticles in the sample were 0.1, 1, and 10 $\mu g.mL^{-1}$. Cells were incubated with nanoparticles at 37 °C for 24 h. Then, cells were observed under Olympus CKX41 optical microscope at a magnification of 400×.

Antimicrobial Activity. The antibacterial activity of the investigated nanoparticles containing titanium dioxide was assayed *in vitro* against three strains of Gram-positive and two Gram-negative bacteria and two strains of yeasts. *Staphylococcus aureus* ATCC 6538, *Staphylococcus epidermidis* ATCC 12228, *Escherichia coli* ATCC 8739, *Pseudomonas aeruginosa* ATCC 27853, and *Candida albicans* ATCC 10231 are strains commonly used for antimicrobial drug discovery testing, but two strains originated from clinics: *S. epidermidis* MRCNS ZMF 12 was methicillin resistant strain isolated from the hospital environment *Candida glabrata* ZMF 40 was isolated from clinical specimen from humans. To determine the antimicrobial activity, the microdilution method according to the CLSI recommendations[42,43] with modifications was used. Serial 2-fold dilutions of dendrimers (500−3.9 $\mu g \cdot mL^{-1}$) in microtiter plates were prepared in Mueller Hinton Broth (BioMaxime) for bacteria and in RPMI-1640 Medium (Sigma) for yeasts and then inoculated with standardized suspensions of microorganisms. After incubation, 24 h for bacteria and 48 h for yeasts, the optical density of medium in 630 nm was measured and compared with non-inoculated medium with dendrimers as a blind probe. Antimicrobial activity was expressed as a percentage of growth of the investigated strain on proper medium without the tested compound. MIC (minimal inhibitory concentration) values were expressed in $\mu g.mL^{-1}$.

Statistical Analysis. The results are presented as mean ± SD. Statistical analysis was performed with the use of the SigmaPlot 11.0

DOI: 10.1021/acsami.5b04780
ACS Appl. Mater. Interfaces 2015, 7, 19994−20003

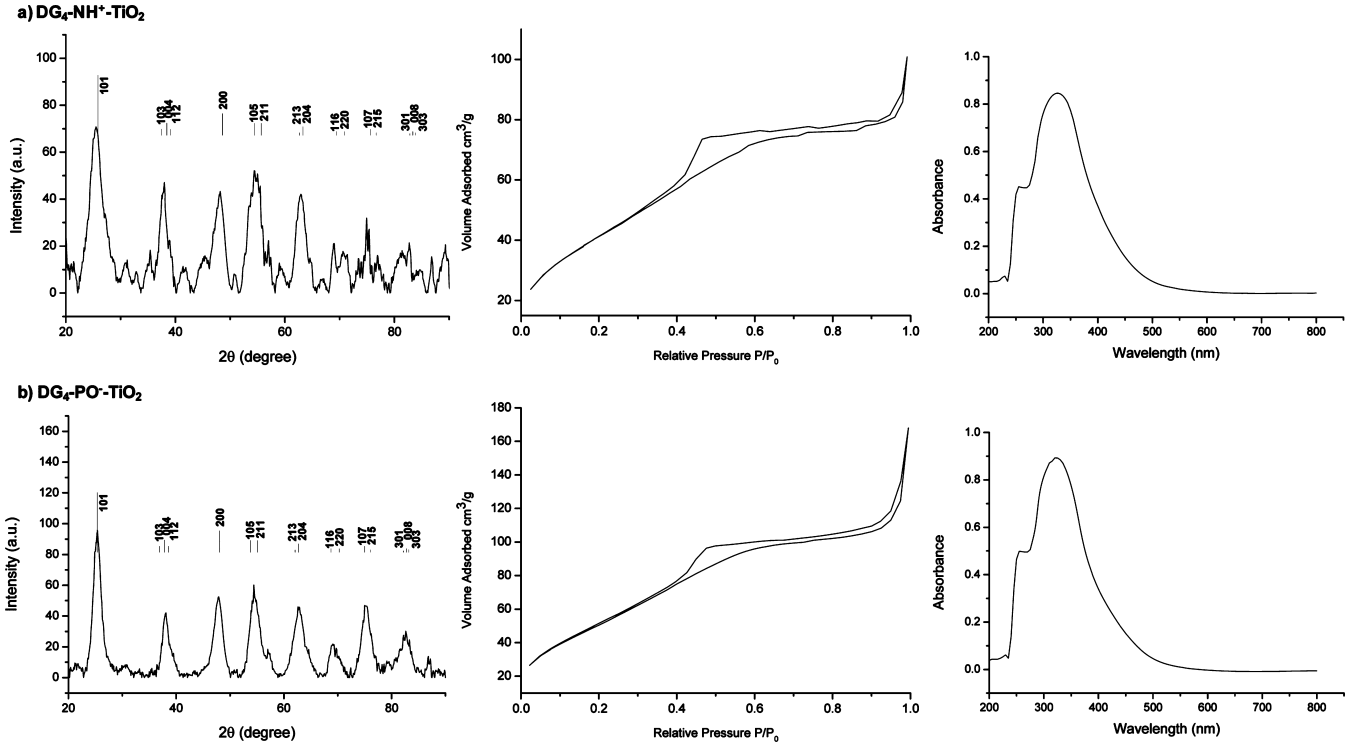

Figure 2. Textural and optical characterization of the dendrimer-coated titanium dioxide materials (a) ammonium-terminated and (b) phosphonate-terminated dendrimer-coated titanium dioxide. From left to right: XRD showing the typical pattern of crystalline anatase. Nitrogen physisorption showing an open mesoporous framework and DRUV showing the absorption region of the hybrid materials.

Systat Software. Statistical evaluation of the difference between control and treated group was performed using Student's t test. $P < 0.05$ and below were accepted as statistically significant.

3. RESULTS AND DISCUSSION

Synthesis and Characterization of the Four Selected Organo-Coated Titanium Dioxide Materials. The sol–gel condensation of the starting titanium alkoxide performed in the presence of the previously mentioned organomodifiers enabled access to novel organic–inorganic hybrid materials (Figure 1). The incorporation of the organomodifier (either dendrimers or branches) within the titanium-oxo-network has been confirmed by CP MAS NMR and DRIFT spectroscopy (S2 and S3 in SI). ^{13}C and ^{31}P NMR showed signals typical of the parent organomodifiers (dendrimers or branches), indicating the preservation of the organic skeletal during titanium alkoxide mineralization. Notably, ^{31}P NMR allowed the discrimination of the phosphorus signal of the core (weak signal around 6 to 8.5 ppm that slightly overlaps with the sideband), those of the branching units (at 60.6 and 69.4 ppm for **DG_4-PO^--TiO_2** and **DG_4-NH^+-TiO_2**, respectively), and last, those located on the surface at 15.59 ppm in the special case of **DG_4-PO^--TiO_2** (S2, SI). Nitrogen physisorption analysis reveals the mesoporous nature of these hybrid materials (Figure 2). The isotherm profiles substantiate an H_2-type hysteresis loop and an interparticular porosity at $P/P_0 > 0.85$. The specific surface areas and pore sizes were estimated to be 158 $m^2\ g^{-1}$ and 3.6 nm for **DG_4-NH^+-TiO_2** and 203 $m^2\ g^{-1}$ and 3.12 nm for **DG_4-PO^--TiO_2** (Table 1).

Small angle X-ray diffraction reveals a single broad peak typical of disordered mesoporous materials (S4, SI). Unexpectedly, although the sol–gel mineralization of titanium tetraisopropoxide was conducted at a low temperature of 60 °C,[44] wide-angle X-ray diffraction analysis reveals a set of well resolved peaks unambiguously attributed to the crystalline anatase phase (Figure 2). The sizes of the crystallites estimated from the half-height widths of the {101} peaks are 4.8 and 5.2 nm for **DG_4-PO^--TiO_2** and **DG_4-NH^+-TiO_2**, respectively. SEM analysis revealed a network built from connected microspheres (Figure 3a). HRTEM analysis and the corresponding selected angle electron diffraction (SAED) pattern corroborated the aforementioned crystalline phase of titanium oxide (Figure 3b,c). Indeed, small crystalline particles appear to be well entangled within the material framework, the lattice fringes of the crystals being assigned to the [101] plane of anatase with a calculated interplanar distance of 3.5 Å typical of the suspected allotrope phase.

By sharp contrast, mineralization of titanium tetraisopropoxide conducted in the presence of either cationic or anionic

Table 1. Physicochemical and Textural Properties of the As-Prepared Materials

material	TiO_2 type	E^a (mV)	$D_H{}^b$ (nm)	$S_{BET}{}^c$ ($m^2.g^{-1}$)	D^d (nm)	size^e (nm)
DG_4-PO^--TiO_2	Anatase	−27.44	421.3	203	3.12	4.8
DG_4-NH^+-TiO_2	Anatase	−22.86	301.4	158	3.6	5.2
B-PO^--TiO_2	Amorphous	−32.59	453.6	376	-	-
B-NH^+-TiO_2	Amorphous	−32.15	441.1	n.m.	-	-

[a]Main value of zeta potential. [b]Hydrodynamic diameter measured by DLS. [c]Specific surface areas of the as-synthesized hybrid materials as determined by nitrogen sorption analysis. [d]Average pore diameter (BJH). [e]Average crystallite size using the Debye–Scherrer equation by X-ray diffraction analysis.

DOI: 10.1021/acsami.5b04780
ACS Appl. Mater. Interfaces 2015, 7, 19994–20003

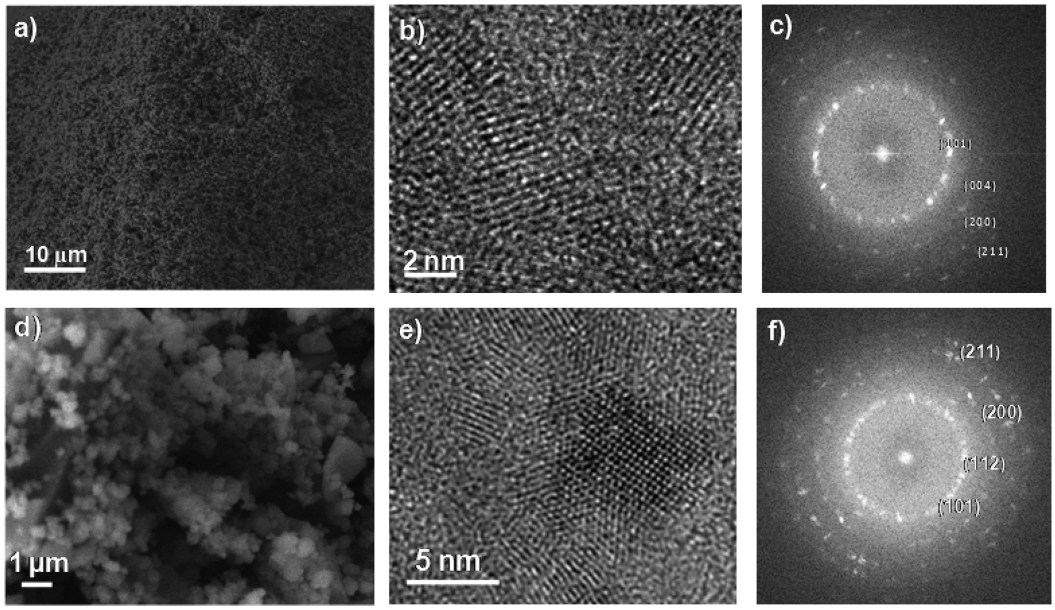

Figure 3. Microscopic analysis of (a–c) DG_4–PO^-–TiO_2 and (d–f) DG_4–NH^+–TiO_2. (a,d) SEM; (b,e) HRTEM; (c,f) SAED.

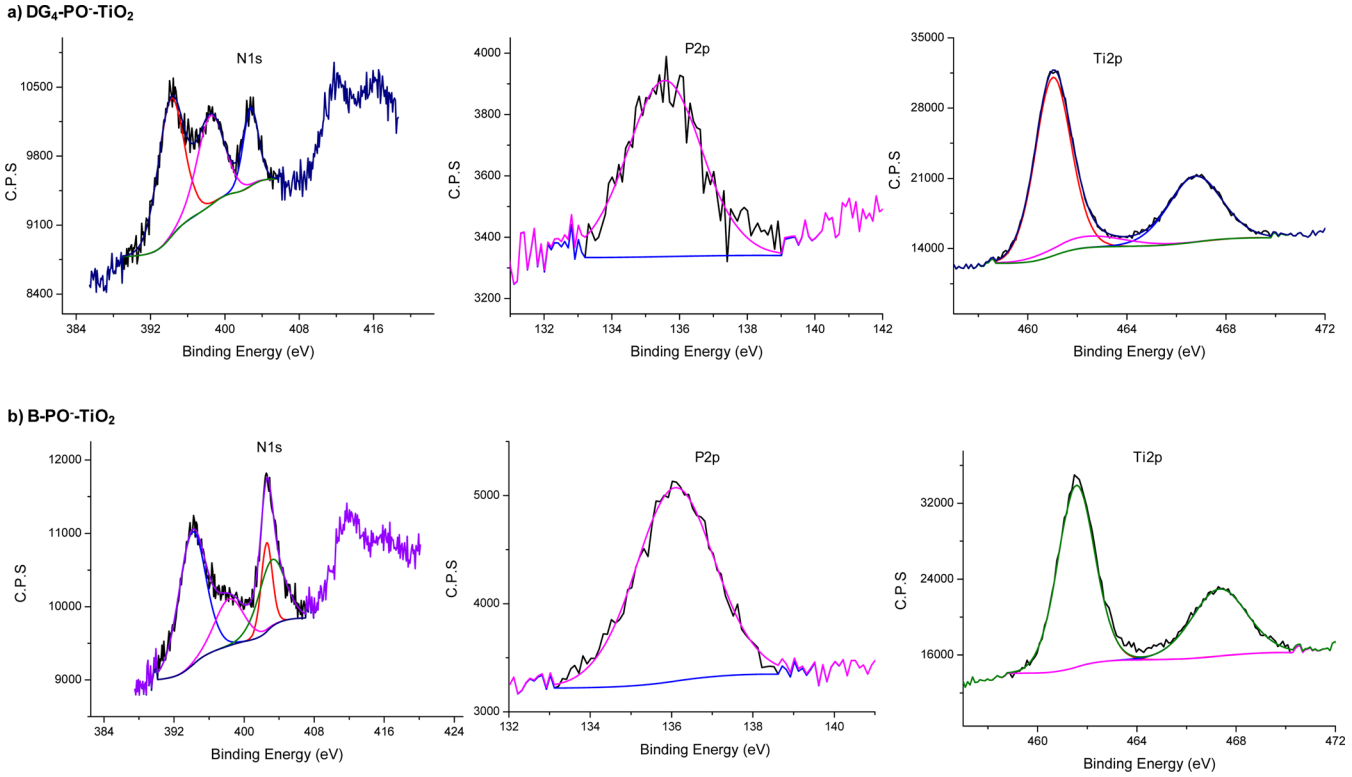

Figure 4. Illustration of the similarities at the interface–surface composition of the dendrimer-coated and branch-coated titanium dioxide ((a) DG_4-PO^--TiO_2 and (b) B-PO^--TiO_2, respectively) by means of XPS analysis. From left to right: binding energy of nitrogen, phosphorus, and titanium elements.

branches (B-NH^+ and B-PO^-) failed to generate any crystalline phase, and only amorphous titanium oxide phase was obtained for both B-NH^+-TiO_2 and B-PO^--TiO_2. This result points to an original dendritic effect exclusive to phosphorus dendrimers emanating most probably from various parameters: First, the unique globular-shaped microstructure, wall flexibility, and swelling behavior of these dendrimers allow the generation of an open porous framework.[45,46] Second, the dendrimer core is built from an extremely hydrophobic cyclotriphosphazene ring, while the peripheries are constructed from polar hydrophilic ammoniums or phosphonates.[32,33] This confers to these dendrimers an amphiphilic character and constitutes a key feature to derive water and polar monomers to the interfacial peripheries creating a strong, rich, and confined environment for the sol–gel nucleation and growth of mineral objects. This mechanistic pathway is somewhat reminiscent of that observed using ionic liquids as a medium during titanium oxide formation.[47]

DOI: 10.1021/acsami.5b04780
ACS Appl. Mater. Interfaces 2015, 7, 19994–20003

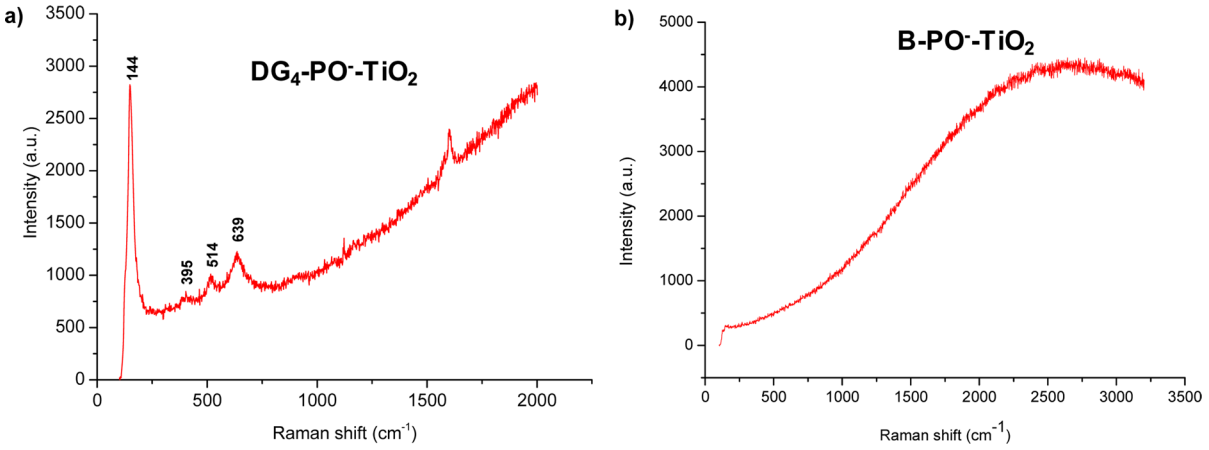

Figure 5. RAMAN spectroscopy of (a) crystalline **DG_4-PO^--TiO_2** and (b) amorphous **B-PO^--TiO_2**.

In the special case of phosphonate-terminated organo-modifiers, further understanding has been gained from XPS analysis in order to elucidate the covalent anchoring at the hybrid interface (Figure 4). The as-synthesized dendrimer–titanium dioxide hybrids exhibit signals with binding energy characteristic of titanium dioxide (461.48 for Ti $2p_{3/2}$ and 467.38 eV for Ti $2p_{1/2}$)[48] thereby excluding the formation of layered titanium phosphate, in perfect consistency with X-ray diffraction. One broad signal is observed for P 2p at 136.12 eV due to the overlap of the binding energy of phosphorus belonging to the surface (phosphonate) and the one located at the core (cyclophosphazene).[49] Three different nitrogen species were also detected at 394.23, 397.93, and 402.63 eV. Exceeding a binding energy value of 401 eV indicates the quaternization of nitrogen element probably by donation to the Lewis acidic titania centers (N → Ti).[48] Similar XPS profiles were recorded for the branch–titanium dioxide hybrid materials as exemplified in Figure 4 (comparison of **DG_4-PO^--TiO_2** and **B-PO^--TiO_2**), illustrating the similarities in the surface–interface composition between the parent **DG_4-PO^--TiO_2** and its **B-PO^--TiO_2** congener.

RAMAN spectroscopic studies were performed on the two categories: the dendrimer–crystalline anatase and the branch–amorphous titanium dioxide. The crystalline **DG_4-PO^--TiO_2** material displays four peaks at values of 144, 395, 514, and 639 cm^{-1}, characteristic of crystalline anatase[49,50] (Figure 5a). In contrast, no crystalline peak has been detected for the fully amorphous **B-PO^--TiO_2** materials (Figure 5b).

UV–visible spectroscopic studies performed on the solid materials reveals the presence of a large band with a maximum at ~320 nm (Figure 2), which is consistent with an incipient oligomerization of Ti(IV) species.[48] The slightly colorful materials (beige) adsorb in the visible region owing most probably to the presence of aromatic rings and electron delocalization within the starting dendrimers that act as sensitizer for anatase particles. Dynamic light scattering (DLS) reveals a hydrodynamic diameter of 421 and 301 nm for **DG_4-PO^--TiO_2** and **DG_4-NH^+-TiO_2**, respectively, and 453 and 441 nm for **B-PO^--TiO_2** and **B-NH^+-TiO_2**, respectively (Table 1). Considering that the size of the crystalline anatase is around 5 nm and that of the **D-G_4** dendrimer is around 7 nm, the corresponding hydrodynamic diameter indicates that each elementary particle is built from an unlimited number of entangled dendrimer-bridged-titanium dioxide that form micro-spherical objects in perfect consistency with SEM analysis. Zeta potential values reveal a higher negative zeta potential (about −32 mV) for branch–amorphous titania compared to their crystalline analogues obtained in **DG_4-NH^+-Ti** (−23 mV) and **DG_4-PO^--Ti** (−28 mV) (Table 1). Notably, owing to the capping of titanium dioxide surface by the organomodifiers (either branches or dendrimers), these hybrid materials can be dispersed in the medium. In contrast, organic-free anatase titanium dioxide strongly aggregates after similar sonication. Its DLS measurement show an average particle size of 1480 nm and a negative zeta potential of −20.4 mV.

Cytotoxicity. Standard MTT cytotoxicity assay revealed that whatever the surface–interface composition and the amorphous or crystalline nature of titanium dioxide, all these hybrid materials caused a concentration-dependent decrease in cell viability. The toxicity was negligible below 10 $\mu g.mL^{-1}$, and in the range of 25 to 100 $\mu g.mL^{-1}$, a statistically significant reduction in viability was noticed (Figure 6). Cytotoxic activity

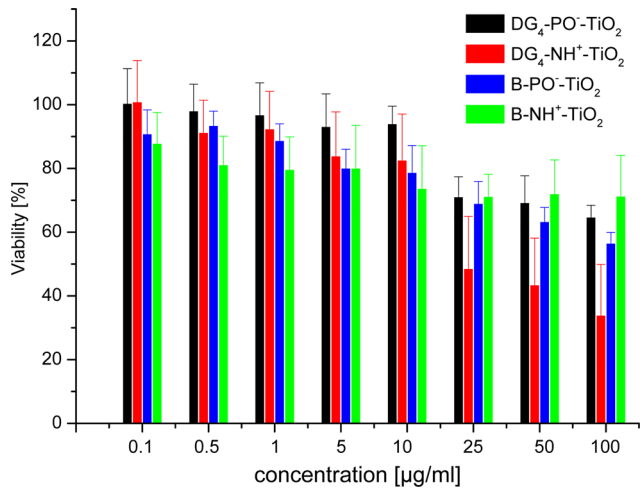

Figure 6. Cytotoxicity of the four hybrid materials after 24 h incubation.

of TiO_2 nanoparticles (crystalline and amorphous) toward human epidermal cells[51] and lymphocytes[52,53] has been previously investigated, and through these studies, it has been shown that these materials display low toxicity for concentration less than 80 $\mu g{\cdot}mL^{-1}$ after incubation times of 6 and 24 h. With concentrations higher than 80 $\mu g.mL^{-1}$, a significant decrease to 60% in cell viability has been observed.[51] In our

DOI: 10.1021/acsami.5b04780
ACS Appl. Mater. Interfaces 2015, 7, 19994–20003

case, after 24 h incubation with the highest concentration of 100 $\mu g \cdot mL^{-1}$, the cell viability ranges from 57% to 71% for **DG_4-PO^--TiO_2**, **B-PO^--TiO_2**, and **B-NH^+-TiO_2**. In contrast, **DG_4-NH^+-TiO_2** revealed high toxicity reducing cell viability to 34% (Figure 6).

The presence of abundant positive amino groups on the surface of **DG_4-NH^+-TiO_2** certainly accounts for its easy interaction with the cell membranes. Previously, the toxic responses of murine embryonic hippocampal cells (mHippoE-18) and neuroblastoma cells (N2a) to treatment with ammonium-terminated phosphorus dendrimers have been substantiated.[54] In that case, the second-generation **DG_2-NH^+** became highly toxic at concentrations above 1 μM and at only 0.7 μM in the case of the third generation **D-G_3-NH^+** for mHippoE-18 cells. The decrease in cell viability has been correlated with disturbances in cellular activities, such as massive ROS generation. In our case, it appears that the toxicity of the ammonium-terminated dendrimers were attenuated upon hybridization with titanium dioxide phase. The resulting hybrid **DG_4-NH^+-TiO_2** has a negative zeta potential of −22.86 mV, whereas the starting **DG_4-NH^+** displays a positive zeta potential of +5 mV. With this negative value, **DG_4-NH^+-TiO_2** can be repelled by the negatively charged cell membrane. The nature of the framework does not induce any specific effect, as similar biological response has been observed for **DG_4-PO^--TiO_2** and **B-PO^--TiO_2** with crystalline and amorphous phase, respectively. The difference seen between **DG_4NH^+-TiO_2** and **B-NH^+-TiO_2** can be attributed to the increasing number of ammonium groups on the terminal position. Their crowded space affords more active cationic sites for interaction with living cells. The general tendency that toxicity of dendrimers becomes intensified with increasing generation seems to be connected to this observed phenomenon.[55] Herein, in **B-NH^+-TiO_2**, all terminated ammoniums are covered by titanium-oxo-layers, while in the case of **DG_4-NH^+-TiO_2**, some ammoniums are suspected to be free for sterical reasons (unmatched zones due to the strain resulting from the well-defined shape of the phosphorus dendrimers and the curvatures created by the polymeric growth of titanium dioxide microspheres).[36]

Hemotoxicity. The nanosize of these hybrid materials facilitates their uptake into cells and their transcytosis across epithelial cells into blood and lymph circulation to reach various organs in the human body. As membrane-bound layer aggregates or single TiO_2 nanoparticles can enter into the cells,[56] we were interested in evaluating the hemotoxicity of these new materials. The obtained results show a statistically significant increase in hemolysis with increasing concentration of the organo-coated titanium dioxide only in the case of **DG_4NH^+-TiO_2**. This relationship was observed after 3 and 24 h of incubation (Figures 7 and S5, SI) in **DG_4NH^+-TiO_2** at the concentration of 100 $\mu g.mL^{-1}$ contributed to the increase of hemolysis to ∼20% after 3 h of incubation and to ∼54% after 24 h. The three other materials caused a statistically significant increase in the level of hemolysis compared to the control for only the two highest concentrations. However, these changes are minor and did not exceed 5% after 24 h of incubation, so they cannot be considered hemolytic at all. In a complementary fashion, changes in the red blood cell shape in response to interactions with these hybrid materials were studied by optical microscopy. Control cells had the shape of discocytes. The presence of 1 and 10 $\mu g.mL^{-1}$ nanoparticles in a cell suspension induced echinocytic transformation. After 24 h of incubation with the concentration ranging from 1 to 10 $\mu g.mL^{-1}$, the

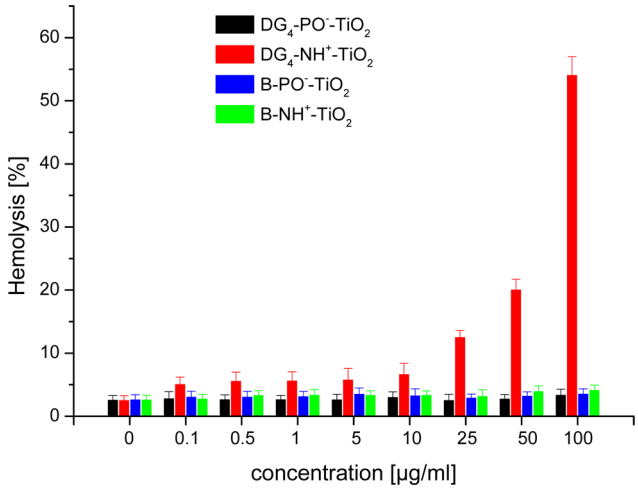

Figure 7. Hemolytic activity of the four hybrid materials.

appearance of the cytoplasmic projections on the surface and the conversion of normal erythrocytes to echinocytes were noticed. At the highest used concentration of 100 $\mu g.mL^{-1}$, many cells were completely deformed, with the appearance of residues from the escape of hemoglobin. The lowest number of normal erythrocytes was observed for **DG_4NH^+-TiO_2** where the hemolysis reached 54% for the highest concentration used. The great difference in hemolysis between **DG_4NH^+-TiO_2** and **DG_4PO^--TiO_2** is illustrated in Figure 8, confirming thereby the

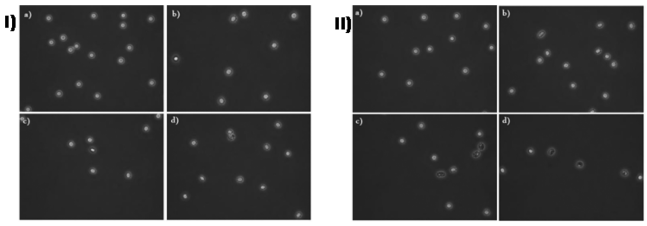

Figure 8. Photographs of control erythrocytes (a); erythrocytes treated at a concentration of 1 $\mu g.mL^{-1}$(b), 10 $\mu g.mL^{-1}$ (c), 100 $\mu g.mL^{-1}$ (d), (magnification, 400×). (I) corresponds to the behavior after treatment with **DG_4PO^--TiO_2** while (II) reflects the results obtained with **DG_4NH^+-TiO_2**.

pivotal role of the functional group in directing the material–cell interactions. The results obtained herein are consistent with the well-established toxicity of ammonium-terminated dendrimers.[57] Indeed, in the case of PAMAM dendrimers, it was proven that the percentage of hemolysis depends on the number of charges on the surface of the particles and their electrostatic interactions. PAMAM dendrimers were also able to change the curvature of the membrane[58] and form holes in it.[59] Consequently, the echinocytic transformation caused by the dendrimers used was more profound, and spheroechinocytes were obtained. In the case of ammonium-terminated phosphorus dendrimers, strong interactions with both the hydrophobic part and the polar headgroup region of the phospholipid bilayer have been suggested and found to be at the basis of decreasing membrane fluidity.[60] By comparison, the results obtained herein indicate that the fruitful association of phosphorus dendrimers and titanium dioxide by the co-condensation approach is of interest to attenuate the well-established hemolytic activity of the ammonium-terminated phosphorus dendrimers.

DOI: 10.1021/acsami.5b04780
ACS Appl. Mater. Interfaces 2015, 7, 19994−20003

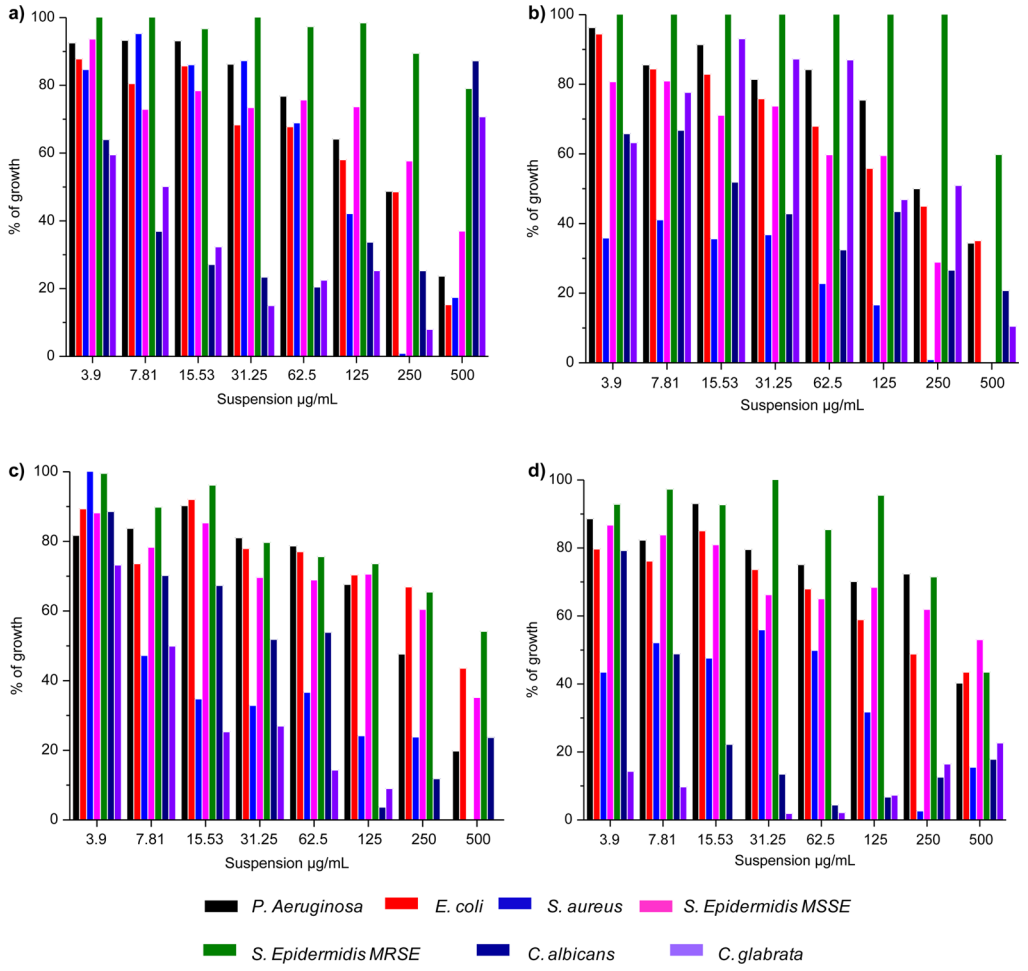

Figure 9. Susceptibility of all investigated bacteria and yeasts to the four organo-coated titanium dioxides: (a) DG_4-PO^--TiO_2, (b) DG_4-NH^+-TiO_2, (c) B-PO^--TiO_2, (d) B-NH^+-TiO_2.

Antimicrobial Activity. Having assessed their cytotoxicity and hemolytical activity, we turned our attention to evaluating the antimicrobial activity of these solid materials. In the concentration range applied here, all of the studied compounds inhibited growth of the tested microorganisms. In most cases, the MIC (minimal inhibitory concentration) value was higher than the highest concentration of the compound used in the study. The studied compounds were not germicidal at the presented concentrations; in all cases the MBC (minimal germicidal concentration) values were higher than MIC. The following materials presented their best activity for yeasts within the range of concentrations: 15.53−250 $\mu g.mL^{-1}$ making the establishment of their MIC values impossible. Notably, their efficiency often decreased when concentration was higher, as illustrated in the case of DG_4-PO^--TiO_2, but also in case of B-PO^--TiO_2 that was revealed as the best material acting on yeasts. The growth of *C. glabrata* ZMF40 was totally inhibited at the concentration of 15.53 $\mu g.mL^{-1}$ of the B-NH^+-TiO_2 and 250 $\mu g.mL^{-1}$ of the B-PO^--TiO_2 compounds, while the DG_4-NH^+-TiO_2 has been found to be the least efficient on yeasts (Figure 9 and S6, SI). In relation to the Gram-negative bacteria, the activity of all the tested compounds was similar, with their best acting on the strain *E. coli* ATCC 8739. At the concentration of 250 $\mu g.mL^{-1}$, their growth was inhibited by 50%. The tested materials presented good activity toward *S. aureus* ATCC 6538. DG_4-NH^+-TiO_2 inhibited the growth of this strain at the concentration of as low as 3.9 $\mu g.mL^{-1}$ by around 40%. This activity grew gradually, achieving 100% inhibition at the concentration of 500 $\mu g.mL^{-1}$ (Figure 9). The DG_4-NH^+-TiO_2 compound was the most active in case of *S. epidermidis* ATCC 12228. The weakest activity of the tested materials is presented toward methicillin-resistant strain of *S. epidermidis* ZMF 12 (MRSE) isolated from the hospital environment.

4. CONCLUSIONS

In conclusion, four novel mesoporous organo-coated titanium dioxide hybrid materials were synthesized and fully characterized. The use of phosphorus dendrimers as organo-modifiers affords, after sol−gel mineralization, discrete crystalline anatase nanoparticles of ∼5 nm entangled in a mesoporous network. In contrast, isolated branch-mimicking dendrimers leads to an amorphous titanium dioxide phase. These materials featuring cationic or ammonium charges at the organic−inorganic interface and built from amorphous or crystalline titanium dioxide framework were evaluated for hemolysis, cytotoxicity, and antimicrobial activity. No noticeable discrimination was observed for amorphous and crystalline material. In contrast, hemolysis and cytotoxicity were found to be sensitive to the nature of the interface composition, with the ammonium-terminated dendrimer-coated titanium dioxide (DG_4-NH^+-TiO_2) being the most hemolytic and cytotoxic material.

DOI: 10.1021/acsami.5b04780
ACS Appl. Mater. Interfaces 2015, 7, 19994−20003

However, compared to the native ammonium-terminated dendrimer, the resulting hybrid material displays diminished toxicity because of its surface alteration by the sol−gel polymerization process. Considering the rising interest of phosphorus dendrimers in nanomedicine (both as cargo as well as their activity per se) and the photodynamic therapy of titanium dioxide, this surface-functionalization might be useful for creating new synergistic machinery mechanisms at the cellular level and for tailoring the biological activity of nanosized organic−inorganic hybrid materials.

■ ASSOCIATED CONTENT

Supporting Information

The Supporting Information is available free of charge on the ACS Publications website at DOI: 10.1021/acsami.5b04780.

Chemical structures of dendrimers and branches, NMR spectra and DRIFT of hybrid materials, detailed information on hemotoxicity and antimicrobial activity of hybrid materials (PDF)

■ AUTHOR INFORMATION

Corresponding Author

*E-mail: a.elkadib@ueuromed.org.

Notes

The authors declare no competing financial interest.

■ ACKNOWLEDGMENTS

Jolanta Wojtczuk is warmly acknowledged for technical assistance in the antimicrobial activity testing experiments.

■ REFERENCES

(1) Muhamed, J.; Revi, D.; Joseph, R.; Anilkumar, T. Phenotypic Modulation of Cell Types around Implanted Polyethylene Terephthalate Fabric in Rabbit Muscle. *Toxicol. Pathol.* **2013**, *41*, 497−507.

(2) Long, M.; Rack, H. J. Titanium Alloys in Total Joint Replacement—A Materials Science Perspective. *Biomaterials* **1998**, *19*, 1621−1639.

(3) Connelly, P. R.; Vuong, T. M.; Murcko, M. A. Getting Physical to Fix Pharma. *Nat. Chem.* **2011**, *3*, 692−695.

(4) Rajh, T. Bio-Functionalized Quantum Dots: Tinkering with Cell Machinery. *Nat. Mater.* **2006**, *5*, 347−348.

(5) Kresge, C. T.; Leonowicz, M. E.; Roth, W. J.; Vartuli, J. C.; Beck, J. S. Ordered Mesoporous Molecular Sieves Synthesized by a Liquid-crystal Template Mechanism. *Nature* **1992**, *359*, 710−712.

(6) Beck, J. S.; Vartuli, J. C.; Roth, W. J.; Leonowicz, M. E.; Kresge, C. T.; Schmitt, K. D.; Chu, C. T. W.; Olson, D. H.; Sheppard, E. W. A New Family of Mesoporous Molecular sieves Prepared with Liquid Crystal Templates. *J. Am. Chem. Soc.* **1992**, *114*, 10834−10843.

(7) Hoffmann, F.; Cornelius, M.; Morell, J.; Fröba, M. Silica-Based Mesoporous Organic−Inorganic Hybrid Materials. *Angew. Chem., Int. Ed.* **2006**, *45*, 3216−3251.

(8) Wan, Y.; Zhao. On the Controllable Soft-Templating Approach to Mesoporous Silicates. *Chem. Rev.* **2007**, *107*, 2821−2860.

(9) Gomez-Cerezo, N.; Izquierdo-Barba, I.; Arcos, D.; Vallet-Regi, M. Tailoring the Biological Response of Mesoporous Bioactive Materials. *J. Mater. Chem. B* **2015**, *3*, 3810.

(10) Mamaeva, V.; Sahlgren, C.; Lindén, M. Mesoporous Silica Nanoparticles in Medicine—Recent Advances. *Adv. Drug Delivery Rev.* **2013**, *65*, 689−702.

(11) Rosenholm, J. M.; Sahlgren, C.; Linden, M. Towards Multifunctional, Targeted Drug Delivery Systems Using Mesoporous Silica Nanoparticles - Opportunities & Challenges. *Nanoscale* **2010**, *2*, 1870−1883.

(12) Asefa, T.; Tao, Z. Biocompatibility of Mesoporous Silica Nanoparticles. *Chem. Res. Toxicol.* **2012**, *25*, 2265−2284.

(13) Rajh, T.; Dimitrijevic, N. M.; Bissonnette, M.; Koritarov, T.; Konda, V. Titanium Dioxide in the Service of the Biomedical Revolution. *Chem. Rev.* **2014**, *114*, 10177−10216.

(14) Wu, S.; Weng, Z.; Liu, X.; Yeung, K. W. K.; Chu, P. K. Functionalized TiO_2 Based Nanomaterials for Biomedical Applications. *Adv. Funct. Mater.* **2014**, *24*, 5464−5481.

(15) Chen, T.; Yan, J.; Li, Y. Genotoxicity of Titanium Dioxide Nanoparticles. *J. Food Drug Anal.* **2014**, *22*, 95−104.

(16) Setyawati, M. I.; Tay, C. Y.; Chia, S. L.; Goh, S. L.; Fang, W.; Neo, M. J.; Chong, H. C.; Tan, S. M.; Loo, S. C. J.; Ng, K. W.; Xie, J. P.; Ong, C. N.; Tan, N. S.; Leong, D. T. Titanium Dioxide Nanomaterials Cause Endothelial Cell Leakiness by Disrupting the Homophilic Interaction of VE−Cadherin. *Nat. Commun.* **2013**, *4*, 1673.

(17) Nanayakkara, C. E.; Larish, W. A.; Grassian, V. H. Titanium Dioxide Nanoparticle Surface Reactivity with Atmospheric Gases, CO_2, SO_2, and NO_2: Roles of Surface Hydroxyl Groups and Adsorbed Water in the Formation and Stability of Adsorbed Products. *J. Phys. Chem. C* **2014**, *118*, 23011−23021.

(18) Nowotny, J.; Bak, T.; Sheppard, L. R.; Nowotny, M. K. Reactivity of Titanium Dioxide with Oxygen at Room Temperature and the Related Charge Transfer. *J. Am. Chem. Soc.* **2008**, *130*, 9984−9993.

(19) Yang, X. N.; Cui, F. Y. Stability of Nano-sized Titanium dioxide in an Aqueous Environment: Effects of pH, Dissolved Organic Matter and Divalent Cations. *Water Sci. Technol.* **2013**, *68*, 276−282.

(20) Qi, J.; Ye, Y. Y.; Wu, J. J.; Wang, H. T.; Li, F. T. Dispersion and Stability of Titanium Dioxide Nanoparticles in Aqueous Suspension: Effects of Ultrasonication and Concentration. *Water Sci. Technol.* **2012**, *67*, 147−151.

(21) Chuang, H.-Y.; Chen, D.-H. Catalyst-free Low Temperature Synthesis of Discrete Anatase Titanium Dioxide Anocrystals with Highly Thermal Stability and UVC-cut Capability. *J. Nanopart. Res.* **2008**, *10*, 233−241.

(22) Zhang, H.; Banfield, J. F. Structural Characteristics and Mechanical and Thermodynamic Properties of Nanocrystalline TiO2. *Chem. Rev.* **2014**, *114*, 9613−9644.

(23) Fujishima, A.; Honda, K. Electrochemical Photolysis of Water at a Semiconductor Electrode. *Nature* **1972**, *238*, 37−38.

(24) George, S.; Pokhrel, S.; Ji, Z.; Henderson, B. L.; Xia, T.; Li, L.; Zink, J. I.; Nel, A. E.; Mädler, L. Role of Fe Doping in Tuning the Band Gap of TiO_2 for the Photo-Oxidation-Induced Cytotoxicity Paradigm. *J. Am. Chem. Soc.* **2011**, *133*, 11270−11278.

(25) Lucky, S. S.; Muhammad Idris, N.; Li, Z.; Huang, K.; Soo, K. C.; Zhang, Y. Titania Coated Upconversion Nanoparticles for Near-Infrared Light Triggered Photodynamic Therapy. *ACS Nano* **2015**, *9*, 191−205.

(26) Kondo, J. N.; Domen, K. Crystallization of Mesoporous Metal Oxides. *Chem. Mater.* **2008**, *20*, 835−847.

(27) Li, W.; Wu, Z.; Wang, J.; Elzatahry, A. A.; Zhao, D. A Perspective on Mesoporous TiO_2 Materials. *Chem. Mater.* **2014**, *26*, 287−298.

(28) Fattakhova-Rohlfing, D.; Zaleska, A.; Bein, T. Three-Dimensional Titanium Dioxide Nanomaterials. *Chem. Rev.* **2014**, *114*, 9487−9558.

(29) El Kadib, A.; Finiels, A.; Brunel, D. Sulfonic Acid Functionalised Ordered Mesoporous Materials as Catalysts for Fine Chemical Synthesis. *Chem. Commun.* **2013**, *49*, 9073−9076.

(30) Sharma, K. K.; Asefa, T. Efficient Bifunctional Nanocatalysts by Simple Postgrafting of Spatially Isolated Catalytic Groups on Mesoporous Materials. *Angew. Chem., Int. Ed.* **2007**, *46*, 2879−2882.

(31) Chen, X.; Mao, S. S. Titanium Dioxide Nanomaterials: Synthesis, Properties, Modifications, and Applications. *Chem. Rev.* **2007**, *107*, 2891−2959.

(32) Brahmi, Y.; Katir, N.; Hameau, A.; Essoumhi, A.; Essassi, E. M.; Caminade, A.-M.; Bousmina, M.; Majoral, J.-P.; El Kadib, A. Hierarchically Porous Nanostructures Through Phosphonate-Metal Alkoxide Condensation and Growth Using Functionalized Dendrimeric Building Blocks. *Chem. Commun.* **2011**, *47*, 8626−8628.

DOI: 10.1021/acsami.5b04780
ACS Appl. Mater. Interfaces 2015, 7, 19994−20003

(33) Brahmi, Y.; Katir, N.; Ianchuk, M.; Colliere, V.; Essassi, E. M.; Ouali, A.; Caminade, A.-M.; Bousmina, M.; Majoral, J. P.; El Kadib, A. Low Temperature Synthesis of Ordered Mesoporous Stable Anatase Nanocrystals: The Phosphorus Dendrimer Approach. *Nanoscale* **2013**, *5*, 2850−2856.
(34) Ciepluch, K.; Katir, N.; El Kadib, A.; Felczak, A.; Zawadzka, K.; Weber, M.; Klajnert, B.; Lisowska, K.; Caminade, A.-M.; Bousmina, M.; Bryszewska, M.; Majoral, J. P. Biological Properties of New Viologen-Phosphorus Dendrimers. *Mol. Pharmaceutics* **2012**, *9*, 448−457.
(35) Milowska, K.; Grochowina, J.; Katir, N.; El Kadib, A.; Majoral, J.-P.; Bryszewska, M.; Gabryelak, T. Viologen-phosphorus Dendrimers Inhibit α-Synuclein Fibrillation. *Mol. Pharmaceutics* **2013**, *10*, 1131−1137.
(36) El Kadib, A.; Katir, N.; Bousmina, M.; Majoral, J. P. Dendrimer-silica Hybrid Mesoporous Materials. *New J. Chem.* **2012**, *36*, 241−255.
(37) Macia, E. The Role of Phosphorus in Chemical Evolution. *Chem. Soc. Rev.* **2005**, *34*, 691−701.
(38) Mignani, S.; Kazzouli, S. E.; Bousmina, M.; Majoral, J.-P. Dendrimer Space Concept for Innovative Nanomedicine: A Futuristic Vision for Medicinal Chemistry. *Prog. Polym. Sci.* **2013**, *38*, 993−1008.
(39) Sze, A.; Erickson, D.; Ren, L.; Li, D. Zeta-potential Measurement Using the Smoluchowski Equation and the Slope of the Current−time Relationship in Electroosmotic Flow. *J. Colloid Interface Sci.* **2003**, *261*, 402−410.
(40) Tan, Q. Y.; Wang, N.; Yang, H.; Chen, L.; Xiong, H. R.; Zhang, L. K.; Liu, J.; Zhao, C. J.; Zhang, J. Q. Preparation and Characterization of Lipid Vesicles Containing Uricase. *Drug Delivery* **2010**, *17*, 28−37.
(41) Hansen, M. B.; Nielsen, S. E.; Berg, K. Re-examination and Further Development of a Precise and Rapid Dye Method for Measuring Cell Growth/Cell Kill. *J. Immunol. Methods* **1989**, *119*, 203−210.
(42) *Methods for Dilution Antimicrobial Susceptibility Tests for Bacteria That Grow Aerobically; Approved Standard—Eighth Edition*, M07-A7 7th ed., Vol. *26*, 2006, Clinical and Laboratory Standards Institute, Wayne, PA.
(43) Wikler, M. A. (2008) *Reference Method for Broth Dilution Antifungal Susceptibility Testing in Yeasts; Approved standard*, M27-A3 3rd ed., Vol. *28*, Clinical and Laboratory Standards Institute, Wayne, PA.
(44) El Kadib, A.; Bousmina, M. Chitosan Bio-Based Organic−inorganic Hybrid Aerogel Microspheres. *Chem. - Eur. J.* **2012**, *18*, 8264−8277.
(45) Astruc, D.; Boisselier, E.; Ornelas, C. Dendrimers Designed for Functions: From Physical, Photophysical, and Supramolecular Properties to Applications in Sensing, Catalysis, Molecular Electronics, Photonics, and Nanomedicine. *Chem. Rev.* **2010**, *110*, 1857−1959.
(46) Crooks, R. M.; Zhao, M.; Sun, L.; Chechik, V.; Yeung, L. K. Dendrimer-encapsulated Metal Nanoparticles: Synthesis, Characterization, and Applications to Catalysis. *Acc. Chem. Res.* **2001**, *34*, 181−190.
(47) Zhou, Y.; Antonietti, M. Synthesis of Very Small TiO2 Nanocrystals in a Room-Temperature Ionic Liquid and Their Self-Assembly toward Mesoporous Spherical Aggregates. *J. Am. Chem. Soc.* **2003**, *125*, 14960−14961.
(48) El Kadib, A.; Molvinger, K.; Guimon, C.; Quignard, F.; Brunel, D. Design of Stable Nanoporous Hybrid Chitosan/Titania as Cooperative Bifunctional Catalysts. *Chem. Mater.* **2008**, *20*, 2198−2204.
(49) Zheng, R.; Lin, L.; Xie, J.; Zhu, Y.; Xie, Y. State of Doped Phosphorus and Its Influence on the Physicochemical and Photocatalytic Properties of P-doped Titania. *J. Phys. Chem. C* **2008**, *112*, 15502−15509.
(50) Periyat, P.; Leyland, N.; McCormack, D. E.; Colreavy, J.; Corr, D.; Pillai, S. C. Rapid microwave synthesis of mesoporous TiO_2 for electrochromic displays. *J. Mater. Chem.* **2010**, *20*, 3650−3655.
(51) Shukla, R. K.; Sharma, V.; Pandey, A. K.; Singh, S.; Sultana, S.; Dhawan, A. ROS-mediated Genotoxicity Induced by Titanium Dioxide Nanoparticles in Human Epidermal Cells. *Toxicol. In Vitro* **2011**, *25*, 231−241.
(52) Ghosh, M.; Bandyopadhyay, M.; Mukherjee, A. Genotoxicity of Titanium Dioxide (TiO_2) Nanoparticles at two Trophic Levels: Plant and Human lLymphocytes. *Chemosphere* **2010**, *81*, 1253−1262.
(53) Ghosh, M.; Chakraborty, A.; Mukherjee, A. Cytotoxic, Genotoxic and the Hemolytic Effect of Titanium Dioxide (TiO_2) Nanoparticles on Human Erythrocyte and Lymphocyte Cells in Vitro. *J. Appl. Toxicol.* **2013**, *33*, 1097−1110.
(54) Lazniewska, J.; Milowska, K.; Zablocka, M.; Mignani, S.; Caminade, A.-M.; Majoral, J.-P.; Bryszewska, M.; Gabryelak, T. Mechanism of Cationic Phosphorus Dendrimer Toxicity against Murine Neural Cell Lines. *Mol. Pharmaceutics* **2013**, *10*, 3484−3496.
(55) Svenson, S. Dendrimers as Versatile Platform in Drug Delivery Applications. *Eur. J. Pharm. Biopharm.* **2009**, *71*, 445−462.
(56) Gheshlaghi, Z. N.; Riazi, G. H.; Ahmadian, S.; Ghafari, M.; Mahinpour, R. Toxicity and Interaction of Titanium Dioxide Nanoparticles with Microtubule Protein. *Acta Biochim. Biophys. Sin.* **2008**, *40*, 777−782.
(57) Klajnert, B.; Pikala, S.; Bryszewska, M. Haemolytic Activity of Polyamidoamine Dendrimers and the Protective Role of Human Serum Albumin. *Proc. R. Soc. London, Ser. A* **2010**, *466*, 1527−1534.
(58) Zhang, Z.-Y.; Smith, B. D. High-Generation Polycationic Dendrimers Are Unusually Effective at Disrupting Anionic Vesicles: Membrane Bending Model. *Bioconjugate Chem.* **2000**, *11*, 805−814.
(59) Hong, S.; Bielinska, A. U.; Mecke, A.; Keszler, B.; Beals, J. L.; Shi, X.; Balogh, L.; Orr, B. G.; Baker, J. R.; Banaszak Holl, M. M. Interaction of Poly(amidoamine) Dendrimers with Supported Lipid Bilayers and Cells: Hole Formation and the Relation to Transport. *Bioconjugate Chem.* **2004**, *15*, 774−782.
(60) Wrobel, D.; Ionov, M.; Gardikis, K.; Demetzos, C.; Majoral, J.-P.; Palecz, B.; Klajnert, B.; Bryszewska, M. Interactions of Phosphorus-Containing Dendrimers with Liposomes. *Biochim. Biophys. Acta, Mol. Cell Biol. Lipids* **2011**, *1811*, 221−226.

DOI: 10.1021/acsami.5b04780
ACS Appl. Mater. Interfaces 2015, 7, 19994−20003